Millennial-scale variability in the productivity signal from the Alboran Sea record, Western Mediterranean Sea

Ana Moreno[a*§], Isabel Cacho[a,b], Miquel Canals[a], Joan O. Grimalt[c] and Anna Sanchez-Vidal[a]

[a]CRG Marine Geosciences, Department of Stratigraphy, Paleontology and Marine Geosciences, Faculty of Geology, University of Barcelona, Campus de Pedralbes, C/Martí i Franqués, s/nº, E-08028 Barcelona, Spain

[b]University of Cambridge, The Godwin Laboratory, Pembroke Street, Cambridge CB2 3SA, U.K.

[c]Department of Environmental Chemistry (ICER-CSIC), Jordi Girona, 18, 08034 Barcelona, Spain

[*]Corresponding author: A. Moreno

[§]Now at: Pyrenean Institute of Ecology, Spanish Research Scientific Council

Apdo. 202, 50080 Zaragoza, Spain

E-mails and fax numbers: amoreno@ipe.csic.es (34 976 716019); isabel@natura.geo.ub.es (34 93 4021340); miquel@natura.geo.ub.es (34 93 4021340); jgoqam@iiqab.csic.es (34 93 2045904); asanchez@natura.geo.ub.es (34 93 4021369)

Abstract

Primary productivity of the Alboran Sea (Western Mediterranean) is reconstructed for the time interval 48,000 to 28,000 years BP using the following geochemical proxies: calcium carbonate, barium excess (Ba_{excess}), total organic carbon (TOC) and alkenone concentration. The records show a consistent pattern that indicates enhanced productivity during Dansgaard/Oeschger (D/O) warm periods. At the same time, deep-water conditions were favorable for organic matter preservation in the sediments, as indicated by the variation in redox-sensitive elements, such as Mn, Cr or V, and by the $\delta^{13}C$ record of benthic foraminifers. The Alboran Sea productivity variation during D/O cycles is explained by the succession of two climatic scenarios that led to latitudinal shifts of the westerly wind system. This mechanism would also account for the variability in the deep-water ventilation of the Western Mediterranean Sea.

Keywords

Paleoproductivity, Western Mediterranean, deep-water, D/O variability, geochemistry

1. Introduction

Paleoclimate studies have revealed high-frequency climatic instabilities during the Latest Pleistocene on millennial to centennial time-scales, the Dansgaard/Oeschger cycles (D/O) and Heinrich Events (HE) (Bond et al., 1993; Dansgaard et al., 1993). These climate fluctuations are present in numerous marine and continental records from all over the world (see compilations in Leuschner and Sirocko, 2000; Voelker, 2002), thus demonstrating the existence of a global climatic signal, but the causes behind this variability are not well understood (Labeyrie and Elliot, 1999; Sarnthein et al., 2002). Therefore, it becomes increasingly important to better constrain the underlying mechanisms that drove the D/O cycles and to assess the potential linking between distinct processes at different latitudes. High-resolution proxy profiles from marine cores that record both paleooceanographic and atmospheric processes are necessary to accomplish this purpose since they help to overcome the dating uncertainties that are usually encountered in studies where such records are derived from different cores or archives.

In the last few years, several high-resolution paleoceanographic studies have been carried out in the Western Mediterranean Sea, and demonstrated a pronounced sensitivity of this basin to high-latitude millennial-scale climate variability (e.g. Krigjsman, 2002). In particular, IMAGES (International Marine Global Change Studies) core MD95-2043 from the Alboran Sea has been intensively studied and provides evidence for surface polar water invasions from the Atlantic during HE (Cacho et al., 1999). An atmospheric mechanism is invoked to explain both the variability of sea surface temperature (SST) and deep-water formation in the western Mediterranean that occurred at the pace of the D/O climatic cycles (Cacho et al., 2000). In addition, pollen records from the same core document significant vegetation shifts on the surrounding continents (Sánchez-Goñi et al., 2002) while strong changes in fluvial and aeolian inputs imply increased aridity in southeastern Iberia and stronger Saharan winds during cold stadial periods (Moreno et al., 2002).

In this complementary study we assess in detail the response of marine productivity to climate and hydrological changes in the Alboran Sea. Paleoproductivity records may provide valuable information about the variability in the regional wind pattern and strength because primary productivity at this location depends on the strength of wind-driven upwelling of nutrient-rich subsurface waters (Garcia-Gorriz and Carr, 2001). Records of TOC and long chain alkenones from the IMAGES core MD95-2043 were presented in a previous study (Cacho et al., 2000) but their interpretation in terms of paleoproductivity was limited by the lack of independent control on the influence of coeval changes in deep water ventilation and their effect on organic carbon preservation. Our new study combines (i) paleoproductivity proxies, such as calcium carbonate, TOC, alkenones and barium excess (Ba_{excess}), and (ii) redox-sensitive elements. Downcore variation in redox-sensitive elements, e.g. Mn, V, Cr, Mo, Ni or Co, likely indicate deep-water ventilation at the time of sedimentation for the time interval between 28 and 48 kyr BP (i.e. Calvert and Pedersen, 1993). This multi-proxy approach allows separating real paleoproductivity signals from those that are altered by diagenetic modifications. From this we gain, first, a better understanding of the environmental conditions over the last glacial cycle in the Alboran Sea and, second, new insight into the linking between biological productivity and millennial-scale climatic variations.

2. Environmental setting

2.1.- Core location and present-day oceanography

Core MD95-2043 was retrieved in the Alboran Sea, the westernmost basin in the Mediterranean Sea, (36º 8.6'N; 2º 37.3'W; 1841 m water depth) during the 1995 IMAGES-I Calypso coring campaign onboard R/V Marion Dufresne (Figure 1). Three water masses fill this basin. The surface layer is formed by Modified Atlantic Water (MAW) that describes a quasi-permanent anticyclonic gyre in the west, the Western Alboran Gyre (WAG) and a more variable circuit in the east, the Eastern Alboran Gyre (EAG) (Millot, 1999; Perkins et al., 1990). The intermediate water is an extension of the Levantine Intermediate Water (LIW) formed in the Eastern Mediterranean (Parrilla et al., 1986). Finally, Western Mediterranean Deep Water (WMDW) fills the deepest layer. WMDW is formed in the Gulf of Lions (Figure 1) where north-westerly winds evaporate and cool surface water until it sinks to the deep basin (Millot, 1999). Deep-water overturning cell in the Gulf of Lions is also fed by the salty LIW. Consequently, formation of WMDW is influenced, to some extent, by the operation way of the overturning cells in the eastern Mediterranean Sea (Pinardi and Masetti, 2000).

In contrast with the rest of the Mediterranean Sea, primary productivity is high in the Alboran Sea where an annual mean of 200 $gCm^{-2}yr^{-1}$ was observed by Antoine et al. (1995). Both wind-induced upwelling, located in the northernmost part of the Western Basin and gyre-induced upwelling along the edges of the anticyclonic gyres (Garcia-Gorriz and Carr, 2001; Sarhan et al., 2000) occur in the Alboran Sea. Although productivity is partially influenced by the interaction between Atlantic and Mediterranean waters (Heburn and La Violette, 1990), over this oceanographic control, other factors have been described in detailed present-day studies (i.e. Vargas-Yáñez et al., 2002). Thus, it is well documented that decreased atmospheric pressure over the Western Mediterranean forces a faster Atlantic inflow that enhances the development of the WAG and a subsequently increase upwelling and marine productivity (Candela and Winant, 1989; García Lafuente et al., 1998; Vargas-Yáñez et al., 2002). Therefore, two main factors influence surface productivity: (i) the speed of the inflowing jet of cold and less-saline surface waters from the Atlantic Ocean that interacts with saltier and warmer waters from the Mediterranean (Perkins et al., 1990), and (ii) westerly winds (so-called *Poniente*) associated with the progression of atmospheric low-pressure centers into the Mediterranean region (Parrilla and Kinder, 1987). Both processes favor the development of anticyclonic gyres that promote upwelling and primary productivity. Additionally, the availability of nutrients via fluvial input further supports high productivity in the Alboran Sea as is clearly evidenced by the close correlation between high chlorophyll concentration and fluvial discharge from southern Iberian rivers (Fabrés et al., 2002).

2.2. Western Mediterranean climate characteristics

At present, summer-time Mediterranean climate is usually dry and hot due to the influence of the atmospheric subtropical high-pressure belt (Sumner et al., 2001). During winter the subtropical high is shifted to the south allowing mid-latitude storms to enter the region from the open Atlantic bringing enhanced amounts of rainfall to the Mediterranean. The present-day precipitation variability in this region on a decadal time-scale has been linked to the North Atlantic Oscillation (NAO) (Goodess and Jones, 2002; Rodó et al., 1997; Sáenz et al., 2001). During low NAO index years, northwesterly winds are weaker and shifted to mid latitudes bringing higher precipitation to the Mediterranean and North African areas. However, during high NAO index years, the strong meridional pressure gradient and the northward shifted position of the surface pressure centers result in the North Atlantic depression tracks that follow a more northerly route and bring humidity to central and northern Europe (Wanner et al., 2001). In addition to this process and particularly during strong winters, the Siberian High extended over Eastern and Central Europe and combined with the Azores High, causes a strong flow over the Mediterranean region thus resulting in very cold and dry winters.

At a centennial to millennial time-scale, abrupt climate change was identified in the Mediterranean region linked to the D/O variability during the last 50,000 yr (Allen et al., 1999; Cacho et al., 1999; Cacho et al., 2000; Combourieu Nebout et al., 2002; Moreno et al., 2002; Paterne et al., 1999; Sánchez-Goñi et al., 2002; Watts et al., 2000). Overall, during cold D/O events (stadials) and HE lower SST and higher aridity were detected, while during warmer periods (interstadials) warmer SST and moister conditions were dominant in the study region. Thus, it was suggested that a prolonged winter anticyclonic stability, probably related to the NAO activity, may be favoured the intensified dryness in the Mediterranean region during cold stadials (Combourieu Nebout et al., 2002; Sánchez-Goñi et al., 2002). In addition, a more vigorous atmospheric circulation over the Western Mediterranean region during D/O stadials was inferred from deep-water convection proxies (Cacho et al., 2000) and Saharan winds intensity indicators (Moreno et al., 2002). The study of paleoproductivity variations in the Alboran Sea at this millennial time-scale will help to test and complete these previously deduced D/O scenarios by determining the relative intensity and displacement of westerly winds which lead productivity variability in the study area.

3. Material and methods

3.1.- Chronostratigraphy

The chronological framework of the core MD95-2043 is described and discussed in Cacho et al. (1999). Two different age models have been developed by these authors that demonstrate a direct correspondence between the D/O climatic variability over Greenland and SST variability in the Alboran Sea. In our study we use the second age model, which cover the core section older than 21,000 yr B.P. and is based on the graphical tuning between the down-core $U^{K'}_{37}$-SST profile (Cacho et al., 1999) and the GISP2 ice core $\delta^{18}O$ curve (Grootes and Stuiver, 1997; Meese et al., 1997). According to this age model the core section studied here, from 1025 to 1585 cm core depth, spans the time interval 28000 and 48000 cal yr B.P. Sedimentation rates are 27 cm/kyr on average resulting in a temporal resolution of 185 years at sampling intervals of 5 cm (Figure 2).

Sedimentation rate values are in general higher during interstadial D/O periods. These variations are probably linked to the higher fluvial input observed during warmer and moister periods (D/O interstadials) (Moreno et al., 2002; Sánchez-Goñi et al., 2002).

3.2.- Geochemical analyses

Major and trace element contents of bulk sediment were analyzed at a sample spacing of 5 cm by means of X-ray fluorescence (XRF). Samples were ground and homogenized in an agate mortar and arranged for elemental determination. For major element measurements, glass discs were prepared by melting about 0.3 g of ground bulk sediment with a Li tetra borate flux. For trace element analyses, discs were prepared by pressing about 5 g of ground bulk sediment into a briquet, with boric acid backing. XRF analyses were performed with a Philips PW 2,400 sequential wave-length dispersive X-ray spectrometer. Analytical accuracy was checked by measuring international standards (GSS-1 to GSS-7) and precision was determined by replicate analyses of samples (0.8% and 4% for major and trace elements, respectively). Variation in the sediment content in redox-sensitive elements, e.g. Mn, Cr, V, Zn, Ni or Cu will indicate deep-water oxygen content at the time of sedimentation for the time interval between 28 and 48 kyr BP in the Alboran

Sea. Thus, Mn forms a highly insoluble oxide where oxic conditions prevail; Cr and V are reduced to insoluble species of lower valency under anoxic conditions, while Zn, Ni or Cu enrichments, without changing their valency, will indicate anoxic bottom waters (Calvert and Pedersen, 1993).

Total carbonate content ($CaCO_3$) was calculated from the total Ca concentration (Ca_{TOT}) obtained by XRF analyses by means of two different approaches (Figure 3b,c). First, we make use of a formula that corrects for clay-derived Ca, which was established for carbonate-rich sediments (1). The original formula from Turekian and Wedepohl (1961) is modified here using the Ca/Al ratio obtained from sediment traps in the Alboran basin. We selected the minimum values of Ca/Al to represent the Calcium associated to terrigenous input.

(1) $CaCO_3 = 2.5\ (Ca_{TOT} - (Ca/Al_{traps} \times Al_{TOT}))$; where Ca/Al_{traps} is 0.21

Second, we calculated the carbonate content from the percentage of volatiles lost on ignition (% LOI) using a correction for dolomite production. Both methods lead to different values, but the structure of both down-core records is essentially identical ($r^2 = 0.9786$) (Figure 3c). The offset between both methods is constant and probably related to the presence of dolomite that was not corrected for in the first approach.

Several studies have demonstrated that barite ($BaSO_4$) and barium (Ba) have a strong association with surface water productivity and they have been used as productivity proxies (e.g. Gingele et al., 1999). Nevertheless, the use of Ba as a record of productivity is constrained by terrigenous Ba input and possible diagenetic remobilization (McManus et al., 1998; Paytan et al., 1996; Schenau et al., 2001). In order to assess the amount of Ba that originates from “biogenic barite”, we corrected the total Ba (Ba_{TOT}) obtained by XRF analyses for the non-biogenic portion that was obtained after geochemical analyses in present-day sediment traps located in the Alboran Sea. From that study, the minimum Ba/Al value of all sediment trap samples was taken as an indicator of the terrigenous sediments (2):

(2) $Ba_{excess} = Ba_{TOT} - (Ba/Al_{minimum} \times Al_{TOT})$; where $Ba/Al_{minimum} = 0.0033$

We have compared it with the results following the more general and widely used Dymond et al. (1992) calculation. Although both barium values and trends are independent of the approach used, we selected the first calculation since it is derived from our study area. Similar Ba/Al values have been determined for the Western Mediterranean Sea (e.g. $Ba/Al_{aluminosilicates} = 0.002$ in Weldeab et al., 2003) and in recent global estimations (0.0037 in Reitz et al., 2004). However, the precipitation of biogenic barium through the water column cannot be evaluated in this sort of approaches. In this paper, we will refer to the corrected barium as barium excess (Ba_{excess}) instead of biogenic barium since the effect of diagenetic remobilization should be discarded before considering this proxy as a paleoproductivity indicator.

In order to avoid dilution effect we present and discuss Element/Al ratios or Mass Accumulation Rates (MAR) (Calvert and Pedersen, 1993; Rollinson, 1993) (Figures 3 and 4). In addition, elemental concentrations and ratios from the literature and values from a study based on sediment traps in the Alboran Sea are used to help in detecting potential diagenetic enrichments in our records due to changes in the water column or porewater redox conditions (Table 1).

4. Results and discussion

4.1.- Paleoproductivity signal

Calcium carbonate contents display a similar pattern as the $U^{k'}_{37}$-SST record in core MD95-2043 (Figure 3a,b) with shifts in the carbonate record systematically lagging those in the SST record. Carbonate content of oligotrophic sediments have been used as a proxy for carbonate paleoproductivity since it is recording the abundance of calcareous plankton (e.g. foraminifera and coccolithophores) (Rühlemann et al., 1999a), but dissolution likewise exerts control on carbonate records. However, foraminiferal fragmentation, an independent dissolution estimator, along the core suggests that carbonate dissolution was negligible during D/O stadial periods and HE, and only increased during the interstadials (Sierro et al., 2001). Thus, carbonate contents during the D/O interstadial periods must represent minimum values since a portion of the carbonate that has been deposited has been lost to dissolution. The excellent carbonate preservation during the stadial periods indicates that processes other than carbonate dissolution are responsible for the reduced carbonate contents during these periods. To discern if paleoproductivity variation was the main process that influenced the carbonate record, other proxies are needed for comparison.

Mass accumulation rates (MAR) of TOC, total alkenones and Ba_{excess} (Figure 3d,e,f) have previously been used in numerous studies to obtain paleoproductivity variations; pitfalls and advantages of these proxies as paleoproductivity estimators are discussed there (Dymond et al., 1992; Gingele and Dahmke, 1994; Müller and Suess, 1979; Suess, 1980;

Villanueva et al., 1998; Grimalt et al., 2000). In core MD95-2043 the different paleoproductivity proxy records all follow a coherent pattern that indicates higher productivity during D/O interstadials (Figure 3d,e,f). However, terrestrial input by rivers and wind has been proved to be a likewise important contributor of terrestrial sediments in the region (Moreno et al., 2002). Thus, an influence on the productivity record due to dilution by non-marine sediment components is likely of relevance. Therefore, MAR of the paleoproductivity proxies are plotted instead of percentages to properly consider the impact of varying sedimentation rates, the variation of the bulk density and the likely dilution effect.

Although the processes that lead to the production of barite are still a matter of debate, the increase in marine barite accumulation rates has been proved to be a direct productivity indicator (Gingele and Dahmke, 1994; Martínez-Ruíz et al., 2000). In this study, we calculated Ba_{excess} as an estimated proxy of biogenic barium. Ba_{excess} has been extensively used as a paleoproductivity indicator. Diagenetic influences have to be considered before using Ba_{excess} record as a productivity proxy. The burial rate of particulate organic matter in highly productive areas may exceed the rate of replenishment of dissolved oxygen and lead to the development of an anoxic environment where sulfate reduction occurs. In those sulfate depleted environments dissolution and mobilization of barite might take place. So that Ba_{excess} peaks could result from reprecipitation processes linked to the re-establishment of oxic conditions (De Lange et al., 1994; Kasten et al., 2001; McManus et al., 1998; Torres et al., 1996). Based on these considerations it has been concluded that the use of Ba_{excess} as a paleoproductivity indicator in sulfate depleted environments (Francois et al., 1995; Schenau et al., 2001), such as highly productive nearshore areas (Dymond et al., 1992), is prone to produce artificial signals that are not directly related to changes in paleoproductivity. But even though Ba and TOC follow quite different post-depositional diagenetic pathways, the records of both proxies in our core display a high degree of congruity. In addition, previous studies of the pore water composition in Alboran sediments (Bernasconi, 1999) indicate that sulfate is depleted by bacterial sulfate reduction at depths below 15-50 meters of sediments. Our study is focused in the first 15 meters of MD95-2043 core thus minimizing the influence of sulfate reduction in the Ba record. Based on these observations we suggest that the Ba and TOC signals are primarily derived from productivity and that diagenesis does not play a major role in defining the structure of the records. However, our hypothesis of using Ba record as a paleoproductivity proxy will be tested using the down-core analyses of redox-sensitive elements that enable to further constrain whether or not post-depositional diagenesis may have occurred.

4.2. Deep-water conditions

Results of $\delta^{13}C$ measured in the benthic foraminifer *Cibicidoides spp*. (mainly *Cibicidoides pachyderma*) were previously published by Cacho et al. (2000). We present here an updated $\delta^{13}C$ profile (Fig. 4a) with higher resolution than the previously published. These results were interpreted to reflect changes in deep-water oxygenation driven by the intensity of the WMDW overturning in the Gulf of Lions (Cacho et al., 2000). In this context, the high $\delta^{13}C$ recorded during stadials (Fig. 4a; reversed axes), in contrast to interstadials, indicates more efficient ventilation of the deep-water mass during these cold intervals. According to our previous statement (section above) organic matter flux increased during interstadials. Thus, the less oxygenated conditions at the benthic layer may reflect oxygen consumption driven by degradation processes of the organic matter. In this case, the benthic $\delta^{13}C$ record in MD95-2043 should be interpreted as a local Alboran productivity signal rather than a whole Western Mediterranean signal for deep basin convection. Over the considered time period, *Cibicidoides pachyderma/kullembergy* were present throughout the investigated core section. These are epibenthic species which prefer relatively low flux rates of carbon and thus are considered good indicators for global signals of deep-water ventilation (Altenbach and Sarnthein, 1989). Apparently, the high productivity Alboran Sea intervals did not transfer high enough carbon fluxes to prevent the presence of these species. For the high productive African coastal areas, it has been estimated that organic matter oxidation could account for up to a ~4-5‰ depletion in the benthic $\delta^{13}C$ record (Sarnthein et al., 1988). Alboran $\delta^{13}C$ oscillations were relatively large (~8-6‰) for a primary productivity system of a far lower magnitude. Consequently we reaffirm the previous interpretation by Cacho et al. (2000) where benthic $\delta^{13}C$ record is considered to reflect mainly changes in the operation mode of the Western Mediterranean deep-water formation. This interpretation was further supported by the parallel covariance of benthic $\delta^{13}C$ and $\delta^{18}O$ records, suggesting the presence of a deep-water mass of distinctive properties between stadial and interstadials (Cacho et al., 2000).

To further explore the magnitude of these changes in deep-water ventilation and to evaluate the potential interference of preservational conditions on the Ba_{excess} record linked to the deep-water conditions redox-sensitive trace elements are presented. As a first approach, we have compared our average geochemical ratios to those from shale composition (Post-Archean Average Shale, PAAS). PAAS values are frequently used as a reference to characterize the composition of the aluminosilicate detritus (Turekian and Wedepohl, 1961; Wedepohl, 1971) (Table 1). In order to provide local values that can represent the original supply to the basin without the effect of diagenetic modifications, we have added sediment trap results from the Alboran Sea to Table 1. Thus, averaged values of selected elements from the sediment traps study are shown to be compared with our average geochemical ratios from MD95-2043 core. We further use data from Cariaco Trench sediments (Calvert and Pedersen, 1993) and Mediterranean sapropels (Wehausen and Brumsack, 2000) as a reference for elemental ratios in sediments that were deposited under suboxic to anoxic conditions. In Table 1, the absence of enrichments of Cu, Cr, V, Ni or Co mean values in the Alboran core is conclusive from the comparison with PAAS values and sediment traps data. This absence further supports that sedimentation occurred under oxygenated bottom water conditions (Calvert and Pedersen, 1993). In addition, we calculated Ni/Co and V/Cr, elemental ratios that are frequently used in the literature to infer anoxic conditions (Jones and Manning, 1994; Martínez-Ruíz et al., 2000). Low values of these ratios in the Alboran core support our hypothesis.

Besides the mean elemental values displayed in Table 1, down-core profiles of analyzed redox-sensitive elements allow the investigation of the deep-water oxygenation for the studied time period (Figure 4). The down-core Cu/Al, Cr/Al and V/Al elemental ratios (Figure 4b, 4c, 4d) remain below the average composition of shales. However, Zn/Al values (Figure 4e) are higher than mean shale composition but still remain well below typical anoxic basin values, if we compare with values presented in Table 1. Mn/Al ratio is above mean PAAS values in some D/O interstadial periods (Figure 4f) indicating occasional enrichments of this element. Cu/Al, Cr/Al and V/Al records do not follow the

D/O pattern marked by the paleoproductivity proxies (Figure 3d,e,f) or the deep-water ventilation indicators (Figure 4a). Therefore, a different origin of these elements is suggested. Cr and V correlate with Al (%) (r^2 = 0.7), an element that does not respond to redox variations thus indicating a possible primarily detrital origin of Cr and V (Morford and Emerson, 1999). On the other hand, Zn and Cu behave as micronutrients, so that are commonly associated to the flux of organic matter (Calvert and Pedersen, 1993). Zn has been particularly linked with the presence of diatoms and its incorporation into their skeletons (Smetacek, 1985) thus explaining its correlation with Ba_{excess} in the Alboran record (Figure 3f).

Mn enrichment commonly has been linked with post-anoxic increases in bottom-water oxygen content (De Lange et al., 1994). Mn is supplied to the ocean as oxide coatings on particulate material delivered by wind or rivers and by diffusion from shelf sediments. This element is dissolved in the water column reaching a maximum at intermediate-depth when oxygen concentrations fall below 100 μM (Calvert and Pedersen, 1993). Dissolved Mn is also present below the oxyhydroxide horizon in the sediments from high-productivity areas where oxygen is consumed at very shallow sediment depths. Solid phases of Mn in these sediments appear as a result of upward diffusion of dissolved Mn and its posterior precipitation at oxic horizons in the form of Mn oxides (Thomson et al., 1987). Our record presents enriched Mn/Al ratios right at the onset of most of the D/O interstadial (Figure 4f). But only three of those Mn/Al peaks go beyond the PAAS values: at the beginning of D/O interstadials 11, 8 and 7. According to the benthic $\delta^{13}C$ record (Figure 4a), the observed Mn/Al enrichments occur just after the maximum oxygen concentrations in deep water thus pointing to a possible link with the Alboran redox variability.

Overall, we conclude that bottom water oxygen concentrations in the Alboran Sea were high enough to prevent extensive sulfate reduction and the remobilization of Ba over the entire studied period. Consequently, our Ba_{excess} record can be used as a reliable paleoproductivity proxy. The combined picture from the carbonate, TOC, Ba_{excess} and alkenone records consistently supports primary productivity oscillations in the Alboran Sea occurring at the D/O frequency which resulted on higher values during the interstadial in relation to the stadial periods.

4.3.- Mechanisms involved in the D/O variability of the Alboran productivity record

In agreement with the present day oceanography of the Western Mediterranean Sea we consider that the D/O variability in Alboran productivity may have been consequence of changes in atmospheric pressure distribution and river runoff regime (see section 2). Our multi-proxy results show solid evidences for enhanced primary productivity during D/O interstadials (Figure 3) and we argue that this situation was mainly the result of two combined processes that may occur along these warmer periods:

(1) Nutrient fertilization induced by enhanced surface water mixing associated with an energetic inflow jet of Atlantic water, presumably resulting from stable low atmospheric pressure over the Western Mediterranean Sea.

(2) Establishment of a wetter climate in the neighbouring land and consequently enhanced nutrient supply by increased river runoff into the Alboran Sea.

In a D/O interstadial situation, North Atlantic Deep Water (NADW) formation took place in the Nordic Seas like at present-day and thus, the SST gradient along the North Atlantic was probably lowered. We therefore suggest that during this "warm scenario" the westerlies were likely weaker and displaced southwards providing higher humidity to the Mediterranean region. In that way, productivity would increase in the Alboran Sea because of (i) the higher fluvial supply of nutrients and (ii) the faster inflow of Atlantic waters and westerly-wind-induced upwelling. The southward displacement of the westerly wind system through a D/O cycle is schematically depicted in Figure 5.

Supporting our hypothesis increased precipitation during interstadials has been previously suggested on the basis of (i) ecosystem modelling using transfer-functions that were applied to fossil pollen assemblages and (ii) grain-size and geochemical analyses along the same Alboran core (Moreno et al., 2002; Sánchez-Goñi et al., 2002). In those previous studies, the decrease in steppic pollen, the predominance of finer terrigenous particles and the increase in fluvial source elements (Al and K), point to wetter conditions in the region during the D/O interstadials. Wet conditions during D/O interstadials were demonstrated by marine pollen records from the Mediterranean region and the Western Iberian margin (Combourieu Nebout et al., 2002; Roucoux et al., 2001; Sánchez-Goñi et al., 2002; Sánchez-Goñi et al., 2000). Italian and Greek pollen sequences also report wet interstadial climate (Allen et al., 1999; Tzedakis, 1999; Watts et al., 2000). Therefore, we hypothesize that surface water fertilization by enhanced river runoff during D/O interstadials may be a consequence of humid climatic conditions on a basin-widescale.

It is known from model results obtained recently for the last glacial period that the location and intensity of the deep water overturning in the North Atlantic has varied throughout the Oxygen Isotope Stage 3 (OIS 3): during D/O stadial periods, NADW formation was considerably reduced and only produced south of Iceland (Ganopolski and Rahmstorf, 2001). Therefore, as inferred by Rühlemann et al. (1999b) for the last deglaciation, it is proposed here that the temperature gradient in the North Atlantic Ocean increased during D/O stadials as a consequence of the decreased northward marine heat transport as result of the reduction in the formation of NADW. This intensified gradient may lead to a strengthened zonal circulation with the concomitant enhancement of the north-westerly winds system. In this "cold scenario", aridity conditions were established in the Mediterranean Sea as indicated by paleodata (Allen et al., 1999; Sánchez-Goñi et al., 2002) and high-resolution climate simulations (Barron and Pollard, 2002).

5. Conclusions

Primary productivity in the Alboran Sea oscillated at millennial time scale parallel to the D/O variability of the last glacial period. All proxies considered, carbonate, Ba_{excess}, TOC and total alkenone records, show consistent patterns indicating a general increase of the Alboran productivity during D/O interstadials relative to the stadials. Abundances of redox-sensitive elements indicate that sulfate reduction did not occur in this deep environment and thus no Ba remobilization should be expected. We infer that enhanced and prolonged primary productivity was sustained during interstadials by a southward shift of the westerly winds to the latitude of the Alboran Sea which forced a more intense inflowing of Atlantic surface jet and led to increased gyre-induced upwelling of nutrient rich subsurface water. Additionally, moister conditions on land, as documented by Al (%) and pollen records, may have supplied additional nutrients by enhanced river runoff during interstadials. Thus, we present two different scenarios associated to D/O stadials and interstadials: (i) during D/O stadials the westerly belt was positioned over northern Iberia thus promoting wind-induced cooling and evaporation and, in consequence, a very efficient deep overturning in the Gulf of Lions; (ii) during D/O interstadials the westerly wind belt shifted southward thus stimulating physical upwelling in the Alboran Sea and, in consequence, deep water convection was less effective in the Gulf of Lions.

Acknowledgements

We are grateful to R. Zahn and J. Targarona (University of Barcelona) and F.J. Sierro and M. A. Bárcena (University of Salamanca) for their useful comments to an earlier version of the manuscript. We thank Rolf Wehausen (University of Oldenburg) for supplying the geochemical data from the sapropelic intervals shown in Table 1. This study was supported by the IMAGES programme and a Comissionat d'Universitats i Recerca fellowship to A.M. GRC Geociencies Marines is additionally funded by Generalitat de Catalunya through its excellency research groups programme. I.C. also thanks EC funding (contract H PMF-CT-1999-00402). Financial support from the "Pole Ocean Pole" project is also acknowledged (EVK2-CT-2000-00089).

References

Allen, J. R. M., Brandt, U., Brauer, A., Hubberten, H. W., Huntley, B., Keller, J., Kraml, M., Mackensen, A., Mingram, J., Negendank, J. F. W., Nowaczyk, N. R., Oberhänsli, H., Watts, W. A., Wulf, S., and Zolitschka, B., 1999. Rapid environmental changes in southern Europe during the last glacial period. Nature 400, 740-743.

Altenbach, A. V., and Sarnthein, M., 1989. Productivity record in benthic foraminifera. In: Productivity of the Ocean: Past and Present. W. H. Berger, V. Smetacek, and G. Wefer, Eds, pp. 255-269. John Wiley.

Antoine, D., Morel, A., and André, J. M., 1995. Algal pigment distribution and primary production in the eastern Mediterranean Sea as derived from coastal zone color scanner observations. Journal of Geophysical Research 100, 16193-16209.

Barron, E., and Pollard, D., 2002. High-resoultion climate simulations of oxygen isotope stage 3 in Europe. Quaternary Research 58, 296-309.

Bernasconi, S. M., 1999. Interstitial water chemistry in the Western Mediterranean: results from leg 161. In: Proceedings of the Ocean Drilling Program, Scientific Results. R. Zahn, M. C. Comas, and A. Klaus, Eds, pp. 423-431. Ocean Drilling Program, College Station, TX.

Bond, G., Broecker, W. S., Johnsen, S. J., McManus, J., Labeyrie, L., Jouzel, J., and Bonani, G., 1993. Correlations between climate records from North Atlantic sediments and Greenland ice. Nature 365, 143-147.

Cacho, I., Grimalt, J. O., Pelejero, C., Canals, M., Sierro, F. J., Flores, J. A., and Shackleton, N. J., 1999. Dansgaard-Oeschger and Heinrich event imprints in Alboran Sea temperatures. Paleoceanography 14, 698-705.

Cacho, I., Grimalt, J. O., Sierro, F. J., Shackleton, N. J., and Canals, M., 2000. Evidence for enhanced Mediterranean thermohaline circulation during rapid climatic coolings. Earth and Planetary Science Letters 183, 417-429.

Calvert, S. E., and Pedersen, T. F., 1993. Geochemistry of recent oxic and anoxic marine sediments: implications for the geological record. Marine Geology 113, 67-88.

Candela, J., and Winant, C. D., 1989. Meteorologically forced subinertial flows through the strait of Gibraltar. Journal of Geophysical Research 94, 12667-12679.

Combourieu Nebout, N., Turon, J. L., Zahn, R., Capotondi, L., Londeix, L., and Pahnke, K., 2002. Enhanced aridity and atmospheric high-pressure stability over the western Mediterranean during the North Atlantic cold events of the past 50 k.y. Geology 30, 863-866.

Dansgaard, W., Johnsen, S. J., Clausen, H. B., Dahl-Jensen, D., Gundestrup, N. S., Hammer, C. U., Hvidberg, C. S., Steffensen, J. P., Sveinbjörnsdóttir, A. E., Jouzel, J., and Bond, G., 1993. Evidence for general instability of past climate from a 250-kyr ice-core record. Nature 364, 218-220.

De Lange, G. J., Van Os, B., Pruysers, P. A., Middelburg, J. J., Castradori, D., Van Santvoort, P., Müller, P., Eggenkamp, H., and Prahl, F., 1994. Possible early diagenetic alteration of paleo proxies. In: Carbon Cycling in the Glacial Ocean. R. Zahn, Ed, pp. 225-257. Springer-Verlag. NATO ASI Series.

Dymond, J., Suess, E., and Lyle, M., 1992. Barium in deep-sea sediment: a geochemical proxy for paleoproductivity. Paleoceanography 7, 163-181.

Fabrés, J., Calafat, A., Sánchez-Vidal, A., Canals, M., and Heussner, S., 2002. Composition and spatio-temporal variability of particle fluxes in the Western Alboran Gyre, Mediterranean Sea. Journal of Marine Systems 33-34, 431-456.

Francois, R., Honjo, S., Manganini, S. J., and Ravizza, G. E., 1995. Biogenic barium fluxes to the deep sea: implications for paleoproductivity reconstruction. Global Biogeochem. Cycles 9, 289-303.

Ganopolski, A., and Rahmstorf, S., 2001. Rapid changes of glacial climate simulated in a coupled climate model. Nature 409, 153-158.

García Lafuente, J., Cano, N., Vargas, M., Rubín, J. P., and Hernández-Guerra, A., 1998. Evolution of the Alboran Sea hydrographic structures during july 1993. Deep Sea Research 45, 39-65.

Garcia-Gorriz, E., and Carr, M.-E., 2001. Physical control of phytoplankton distributions in the Alboran Sea: a numerical and satellite approach. Journal of Geophysical Research 106, 16795-16805.

Gingele, F., and Dahmke, A., 1994. Discrete barite particles and barium as tracers of paleoproductivity in South Atlantic sediments. Paleoceanography 9, 151-168.

Gingele, F., Zabel, M., Kasten, S., Bonn, W. J., and Nürnberg, C. C., 1999. Biogenic barium as a proxy for paleoproductivity: methods and limitations of application. In: Use of proxies in paleoceanography: examples from the South Atlantic. G. Fischer, and G. Wefer, Eds, pp. 345-364. Springer-Verlag Berlin Heidelberg.

Goodess, C. M., and Jones, P. D., 2002. Links between circulation and changes in the characteristics of Iberian rainfall. International Journal of Climatology 22, 1593-1615.

Grootes, P., and Stuiver, M. 1997. Oxygen 18/16 variability in Greenland snow and ice with 10^3-to 10^5-year time resolution. Journal of Geophysical Research 102, 26455-26470.

Grimalt, J.O., Rullkötter, J., Sicre, M.-A., Summons, R., Farrington, J., Harvey, H.R., Goñi, M., and Sawada, K., 2000. Modifications of the C_{37} alkenone and alkenoate composition in the water column and sediment: Possible implications for sea surface temperature estimates in paleoceanography. Geochemistry, Geophysics, Geosystems 1, 2000GC000053.

Heburn, G. W., and La Violette, P. E., 1990. Variations in the structure of the anticyclonic gyres found in the Alboran Sea. Journal of Geophysical Research 95, 1599-1613.

Jones, B., and Manning, D. A. C., 1994. Comparison of geochemical indices used for the interpretation of palaeoredox conditions in ancient mudstones. Chemical Geology 111, 111-129.

Kasten, S., Haese, R., Zabel, M., Rühlemann, C., and Schulz, H., 2001. Barium peaks at glacial terminations in sediments of the equatorial Atlantic Ocean - relicts of deglacial productivity pulses? Chemical Geology 175, 635-651.

Krigjsman, W., 2002. The Mediterranean: Mare Nostrum of Earth sciences. Earth and Planetary Science Letters 205, 1-12.

Labeyrie, L., and Elliot, M., 1999. Abrupt climatic changes-Causes and consequences: An introduction. In: Reconstructing Ocean History: A Window into the Future. F. Abrantes, and A. C. Mix, Eds, pp. 73-82. Plenum Plublishers, New York.

Leuschner, D. C., and Sirocko, F., 2000. The low-latitude monsoon climate during Dansgaard-Oeschger cycles and Heinrich Events. Quaternary Science Reviews 19, 243-254.

Martínez-Ruíz, F., Kastner, M., Paytan, A., Ortega-Huertas, M., and Bernasconi, S. M., 2000. Geochemical evidence for enhanced productivity during S1 sapropel deposition in the eastern Mediterranean. Paleoceanography 15, 200-209.

McManus, J., Berelson, W. M., Klinkhammer, G. P., Johnson, K. S., Coale, K. H., Anderson, R. F., Kumar, N., Burdige, D. J., Hammond, D. E., Brumsack, H.-J., McCorkle, D., and Rushdi, A., 1998. Geochemistry of barium in marine sediments: implications for its use as a paleoproxy. Geochimica et Cosmochimica Acta 62, 3453-3473.

Meese, D. A., Gow, A. J., Alley, R. B., Zielinski, G. A., Grootes, P., Ram, M., Taylor, K. C., Mayewski, P. A., and Bolzan, J. F., 1997. The Greenland Ice Sheet Project 2 depth-age scale: Methods and results. Journal of Geophysical Research 102, 26411-26423.

Millot, C., 1999. Circulation in the Western Mediterranean Sea. Journal of Marine Systems 20, 423-442.

Moreno, A., Cacho, I., Canals, M., Prins, M. A., Sánchez-Goñi, M. F., Grimalt, J. O., and Weltje, G. J., 2002. Saharan dust transport and high latitude glacial climatic variability: the Alboran Sea record. Quaternary Research 58, 318-328.

Morford, J. L., and Emerson, S. R., 1999. The geochemistry of redox sensitive trace metals in sediments. Geochimica et Cosmochimica Acta 63, 1735-1750.

Müller, P., and Suess, E., 1979. Productivity, sedimentation rate, and sedimentary organic matter in the oceans- I. Organic carbon preservation. Deep Sea Research I 26A, 1347-1362.

Parrilla, G., and Kinder, T. H., 1987. Oceanografía física del mar de Alborán. Boletín del Instituto Español de Oceanografía 4, 133-165.

Parrilla, G., Kinder, T. H., and Preller, R. H., 1986. Deep and Intermediate Mediterranean water in the western Alboran Sea. Deep Sea Research 33, 55-88.

Paterne, M., Kallel, N., Labeyrie, L., Vautravers, M., Duplessy, J. C., Rossignol-Strick, M., Cortijo, E., Arnold, E., and Fontugne, M., 1999. Hydrological relationship between the

North Atlantic Ocean and the Mediterranean Sea during the past 15-75 kyr. Paleoceanography 14, 626-638.

Paytan, A., Kastner, M., and Chavez, F., 1996. Glacial to interglacial fluctuations in productivity in the Equatorial Pacific as indicated by marine barite. Science 274, 1355-1357.

Perkins, H., Kinder, T., and La-Violette, P., 1990. The Atlantic inflow in the Western Alboran Sea. Journal of Physical Oceanography 20, 242-263.

Pinardi, N., and Masetti, E., 2000. Variability of the large scale general circulation of the Mediterranean Sea from observations and modelling: a review. Palaeogeography, Palaeoclimatology, Palaeoecology 158, 153-173.

Reitz, A., Pfeifer, K., De Lange, G. J., and Klump, J., 2004. Biogenic barium and the detrital Ba/Al ratio: a comparison of their direct and indirect determination. Marine Geology 204, 289-300.

Rodó, X., Baert, E., and Comin, F. A., 1997. Variations in seasonal rainfall in Southern Europe during the present century: relationships with the North Atlantic Oscillation and the El Niño-Southern Oscillation. Climate Dynamics 13, 275-284.

Rollinson, H., 1993. Using geochemical data. Evaluation, presentation, interpretation. Longman Scientific and Technical.

Roucoux, K. H., Shackleton, N. J., de Abreu, L., Schönfeld, J., and Tzedakis, C., 2001. Combined marine proxy and pollen analyses reveal rapid Iberian vegetation response to North Atlantic millennial-scale climate oscillations. Quaternary Research 56, 128-132.

Rühlemann, C., Müller, P., and Schneider, R., 1999a. Organic carbon and carbonate as paleoproductivity proxies: examples from high and low productivity areas of the tropical

Atlantic. In: Use of proxies in Paleoceanography: examples from the South Atlantic. G. Fischer, and G. Wefer, Eds, pp. 1-31. Springer-Verlag, Berlin.

Rühlemann, C., Mulitza, S., Müller, P., Wefer, G., and Zahn, R., 1999b. Warming of the tropical Atlantic Ocean and slowdown of thermohaline circulation during the last deglaciation. Nature 402, 511-514.

Sáenz, J., Rodríguez-Puebla, C., Fernández, J., and Zubillaga, J., 2001. Interpretation of interannual winter temperature variations over southwestern Europe. Journal of Geophysical Research 106, 20641-20651.

Sánchez-Goñi, M. F., Cacho, I., Turon, J. L., Guiot, J., Sierro, F. J., Peypouquet, J.-P., Grimalt, J. O., and Shackleton, N. J., 2002. Synchroneity between marine and terrestrial responses to millennial scale climatic variability during the last glacial period in the Mediterranean region. Climate Dynamics 19, 95-105.

Sánchez-Goñi, M. F., Turon, J. L., Eynaud, F., and Gendreau, S., 2000. European climatic response to millenial-scale changes in the atmosphere-ocean system during the Last Glacial period. Quaternary Research 54, 394-403.

Sarhan, T., García-Lafuente, J., Vargas, J. M., and Plaza, F., 2000. Upwelling mechanisms in the northwestern Alboran Sea. Journal of Marine Systems 23, 317-331.

Sarnthein, M., Kennet, J. P., Allen, J. R. M., Beer, J., Grootes, P., Laj, C., McManus, J., Ramesh, R., 2002. Decadal-to-millennial-scale climate variability-chronology and mechanisms: summary and recommendations. Quaternary Science Reviews 21, 1121-1128.

Sarnthein, M., Winn, K., Duplessy, J. C., and Fontugne, M., 1988. Global variations of surface ocean productivity in low and mid latitudes: influence on CO2 reservoirs of the deep ocean and atmosphere during the last 21.000 years. Paleoceaography 3, 361-399.

Schenau, S. J., Prins, M. A., De Lange, G. J., and Monnin, C., 2001. Barium accumulation in the Arabian Sea: controls on barite preservation in marine sediments. Geochimica et Cosmochimica Acta 65, 1545-1556.

Sierro, F. J., Pérez-Folgado, M., Flores, J. A., Bárcena, M. A., Cacho, I., Shackleton, N. J., and Grimalt, J. O., 2001. Carbonate dissolution variations and Mediterranean thermohaline circulation, MIS3. In: 7th International Conference on Paleoceanography. H. Okada, Ed, pp. 188, Sapporo, Japan.

Smetacek, V., 1985. Role of sinking in diatom life-history cycles: ecological, evolutionary and geological significance. Marine Biology 84, 239-251.

Suess, E., 1980. Particulate organic carbon flux in the oceans surface productivity and oxygen utilization. Nature 288, 260-263.

Sumner, G., Homar, V., and Ramis, C., 2001. Precipitation seasonality in Eastern and Southern coastal Spain. International Journal of Climatology 21, 219-247.

Taylor, S. R., and McLennan, S. M., 1985. “The continental crust: its composition and evolution.” Blackwell Scientific Publications, Oxford, U.K.

Thomson, J., Colley, S., Higgs, N. C., Hydes, D. J., Wilson, T. R. S., and Sorensen, J., 1987. Geochemical oxidation fronts in NE Atlantic distal turbidites and their effects in the sedimentary record. In: Geology and Geochemistry of Abyssal Plains. P. P. E. Weaver, and J. Thomson, Eds, pp. 167-177.

Torres, M. E., Brumsack, H.-J., Bohrmann, G., and Emeis, K. C., 1996. Barite fronts in continental margin sediments: a new look at barium remobilization in the zone of sulfate reduction and formation of heavy barites in diagenetic fronts. Chemical Geology 127, 125-139.

Turekian, K. K., and Wedepohl, K. H., 1961. Distribution of the elements in some major units of the earth's crust. Geological Society of America Bulletin 72, 175-192.

Tyson, R. V., 2001. Sedimentation rate, dilution, preservation and total organic carbon: some results of a modelling study. Organic Geochemistry 32, 333-339.

Tzedakis, C., 1999. The last climatic cycle at Kopais, central Greece. Journal of Geological Society of London 156, 425-434.

Vargas-Yáñez, M., Plaza, F., García-Lafuente, J., Sarhan, T., Vargas, J. M., and Vélez-Belchi, P., 2002. About the seasonal variability of the Alboran Sea circulation. Journal of Marine Systems 35, 229-248.

Villanueva, J., Grimalt, J. O., Labeyrie, L., Cortijo, E., Vidal, L., and Turon, J. L., 1998. Precessional forcing of productivity in the North Atlantic Ocean. Paleoceanography 13, 561-571.

Voelker, A., 2002. Global distribution of centennial-scale records for marine isotope stage (MIS) 3: a database. Quaternary Science Reviews 21, 1185-1212.

Wanner, H., Brönnimann, S., Casty, C., Gyalistras, D., Luterbacher, J., Schmutz, C., Stephenson, D. B., and Xoplaki, E., 2001. North Atlantic oscillation-concepts and studies. Surveys in Geophysics 22, 321-382.

Watts, W. A., Allen, J. R. M., and Huntley, B., 2000. Palaeoecology of three interstadial event during oxygen-isotope Stages 3 and 4: a lacustrine record from Lago Grande di

Monticchio, southern Italy. Palaeogeography, Palaeoclimatology, Palaeoecology 155, 83-93.

Wedepohl, K. H., 1971. Environmental influences on the chemical composition of shales and clays. In: Physics and Chemistry of the Earth. L. H. Ahrens, F. Press, S. K. Runcorn, and H. C. Urey, Eds, pp. 307-331. Pergamon, Oxford.

Wehausen, R., and Brumsack, H.-J., 2000. Chemical cycles in Pliocene sapropel-bearing and sapropel-barren eastern Mediterranean sediments. Palaeogeography, Palaeoclimatology, Palaeoecology 158, 325-352.

Weldeab, S., Emeis, K. C., Hemleben, C., Schmiedl, G., and Schulz, H., 2003. Spatial productivity variations during formation of sapropels S5 and S6 in the Mediterranean Sea: evidence from Ba contents. Palaeogeography, Palaeoclimatology, Palaeoecology 191, 169-190.

Table 1. Trace element average data in this study compared with values from the literature. Sediment trap data resulting from the annual average of three mooring lines, one located in the western Alboran Sea (ALB-1, from Fabrés et al., 2002) and two located in the eastern Alboran Sea (ALB4 and ALB5) are also indicated.

Data	Cu/Al (10^4)	Cr/Al (10^4)	V/Al (10^4)	Zn/Al (10^4)	Mn/Al (10^4)	Ni/Al (10^4)	Co/Al (10^4)	V/Cr	Ni/Co
MD95-2043	2.4-4.3	9-10.8	2.4-10	9-11.5	60-130	3.5-6.5	1.4-2.4	1-1.25	2-3.5
Shale[a]	5.1	10.2	14.8	10.8	96.2	7.7	2.15	1.4	3.5
PAAS[b]	5.3	11.6	15	8.9	85	5.5	2.3	1.36	2.4
Sediment traps[c]	7.52	11.67	14.85	27.21	118.24	7.84	2.17	1.28	4.03
Anoxic basin[d&e]	5.3[d]	13.4[d]	35.8[d]	16.2[d]	31.2[d]	5.8[d]	-	1-4.3[e]	4.3-7[e]
Eastern Mediterranean sapropels[f]	60	50	307	50	184	88	22	6.14	4

[a] Average shale, data from Wedepohl (1971)
[b] Post-Archean Average Shale, data from Taylor and McLennan (1985)
[c] Alboran sediment trap data resulting from the average of three mooring lines.
[d] Cariaco Trench, data from Table 2 in Calvert and Pedersen (1993)
[e] North Sea, data from Jones and Manning (1994)
[f] Average composition of Pliocene sapropelic sediments from the eastern Mediterranean, ODP Site 969 (Wehausen and Brumsack, 2000)

Figure captions

Figure 1.- Location of IMAGES core MD95-2043 in the Alboran Sea. Present-day dominant oceanographic circulation is represented by dashed arrows. Main rivers supplying sediments to this area are indicated.

Figure 2.- Records of (a) $\delta^{18}O$ from GISP2 core (Grootes and Stuiver, 1997; Meese et al., 1997) and (b) $U^{k'}_{37}$-SST (Cacho et al., 1999) and (c) Linear Sedimentation Rates (LSR) for the studied time interval from MD95-2043 core. Note that each change in the LSR record represents an age control point in the age model constructed in Cacho et al. (1999) based on peak to peak correlation of the MD95-2043 SST record with the GISP2 $\delta^{18}O$ profile (correlation coefficient r^2= 0.92). D/O stadials are indicated by shaded bars and D/O interstadials by numbers.

Figure 3.- MD95-2043 age profiles of (a) $U^{k'}_{37}$-SST (Cacho et al., 1999); (b) MAR carbonate (g/m^{2}yr); (c) comparison between both carbonate calculations (using a formula for carbonate-rich sediments and from the amount of lost volatiles; linear trend and r^2 are also indicated); (d) MAR TOC (g/m^{2}yr) (Cacho et al., 2000); (e) MAR total C_{37} alkenones (Cacho et al., 2000) and (f) MAR Ba_{excess} (g/m2yr).

Figure 4. MD95-2043 age profiles of (a) $\delta^{13}C$ *Cibicidoides spp*. (reverse y axis), (b) Cu/Al, (c) Cr/Al, (d) V/Al, (e) Zn/Al and (f) Mn/Al ratios (PAAS and sediment trap values are indicated by dashed lines).

Figure 5. Climatic scenarios inferred for HE and D/O stadial and D/O interstadial periods.

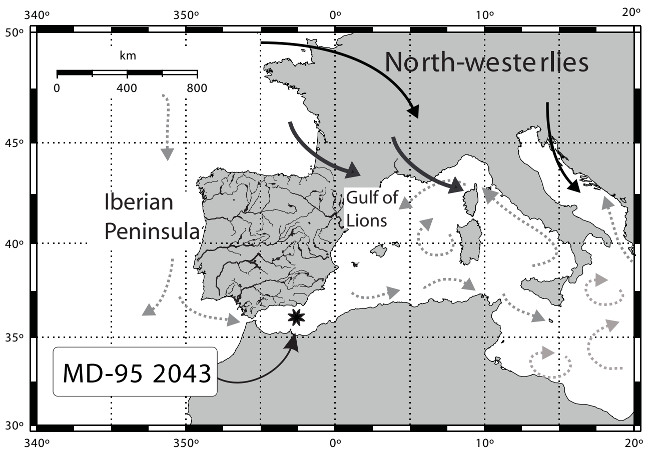

340º
350º
0º
10º
20º
50º
45º
40º
35º
30º
km
0
400
800
North-westerlies
Iberian
Peninsula
Gulf of
Lions
MD-95 2043

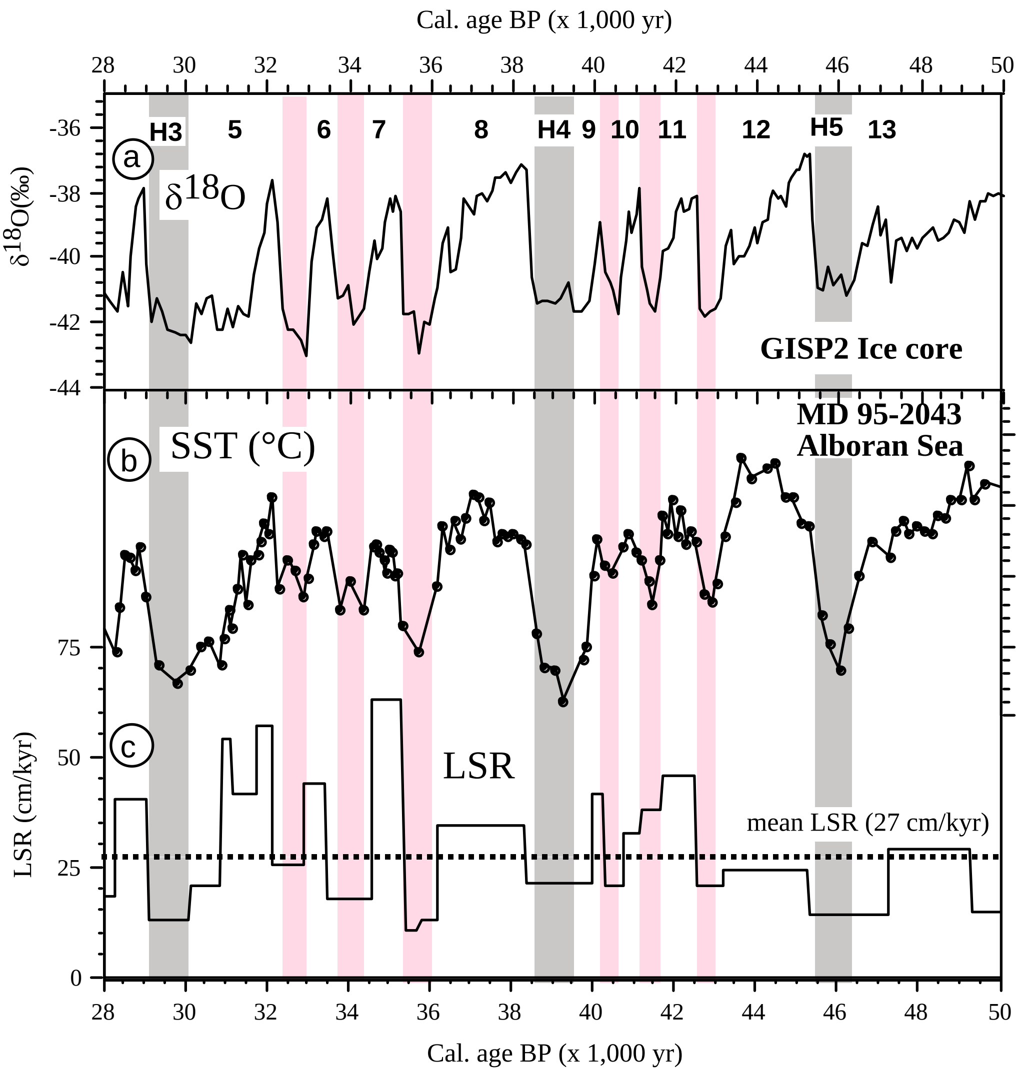

Cal. age BP (x 1,000 yr)
H3
5
6
7
8
H4
9
10
11
12
H5
13
a
δ18O
δ18O(‰)
GISP2 Ice core
MD 95-2043
Alboran Sea
b
SST (°C)
SST (°C)
c
LSR
LSR (cm/kyr)
mean LSR (27 cm/kyr)
Cal. age BP (x 1,000 yr)

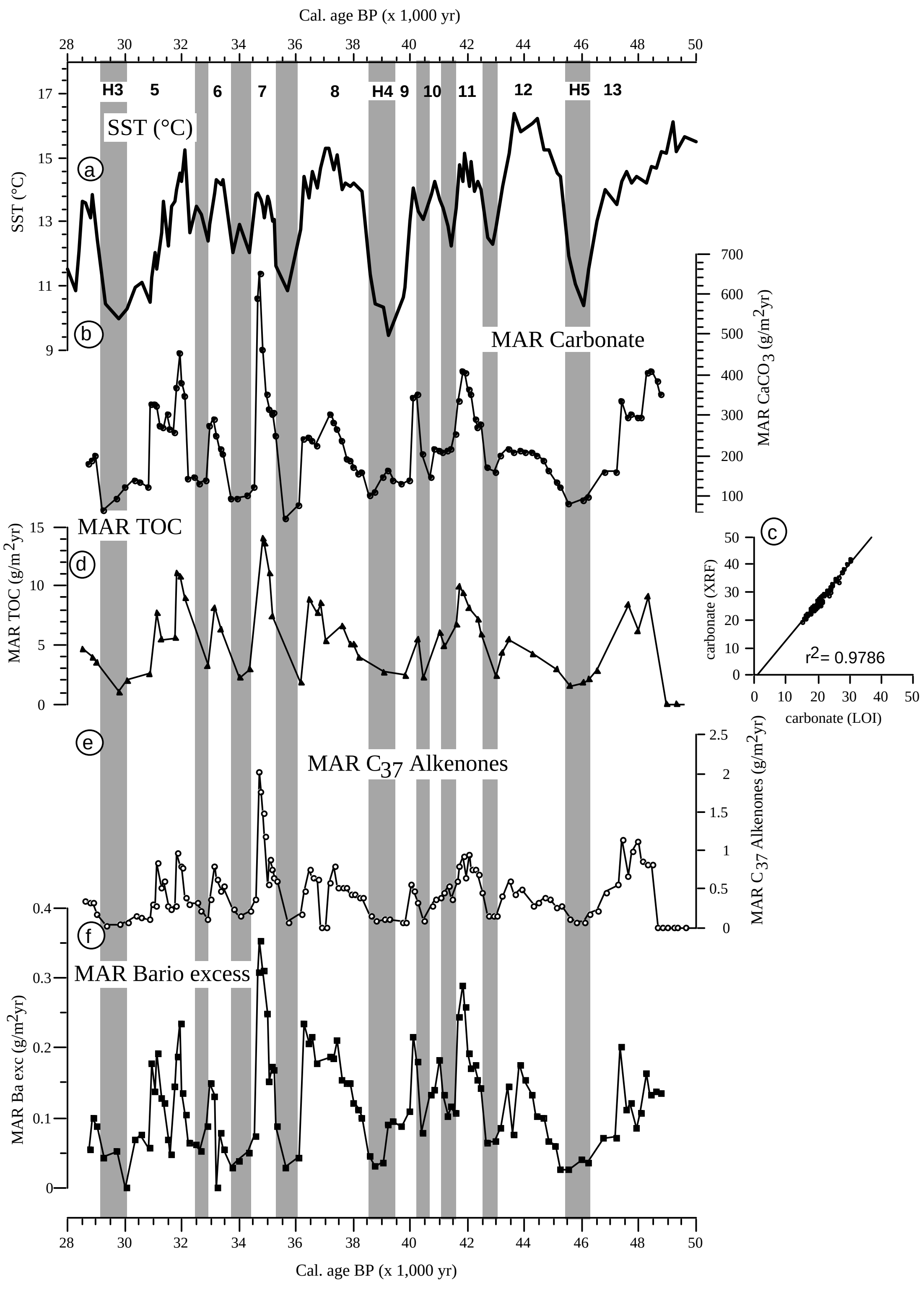
Cal. age BP (x 1,000 yr)
H3
5
6
7
8
H4
9
10
11
12
H5
13
SST (°C)
a
b
c
d
e
f
SST (°C)
MAR Carbonate
MAR $CaCO_3$ (g/m^2yr)
MAR TOC
MAR TOC (g/m^2yr)
carbonate (XRF)
carbonate (LOI)
r^2 = 0.9786
MAR C_{37} Alkenones
MAR C_{37} Alkenones (g/m^2yr)
MAR Bario excess
MAR Ba exc (g/m^2yr)
Cal. age BP (x 1,000 yr)

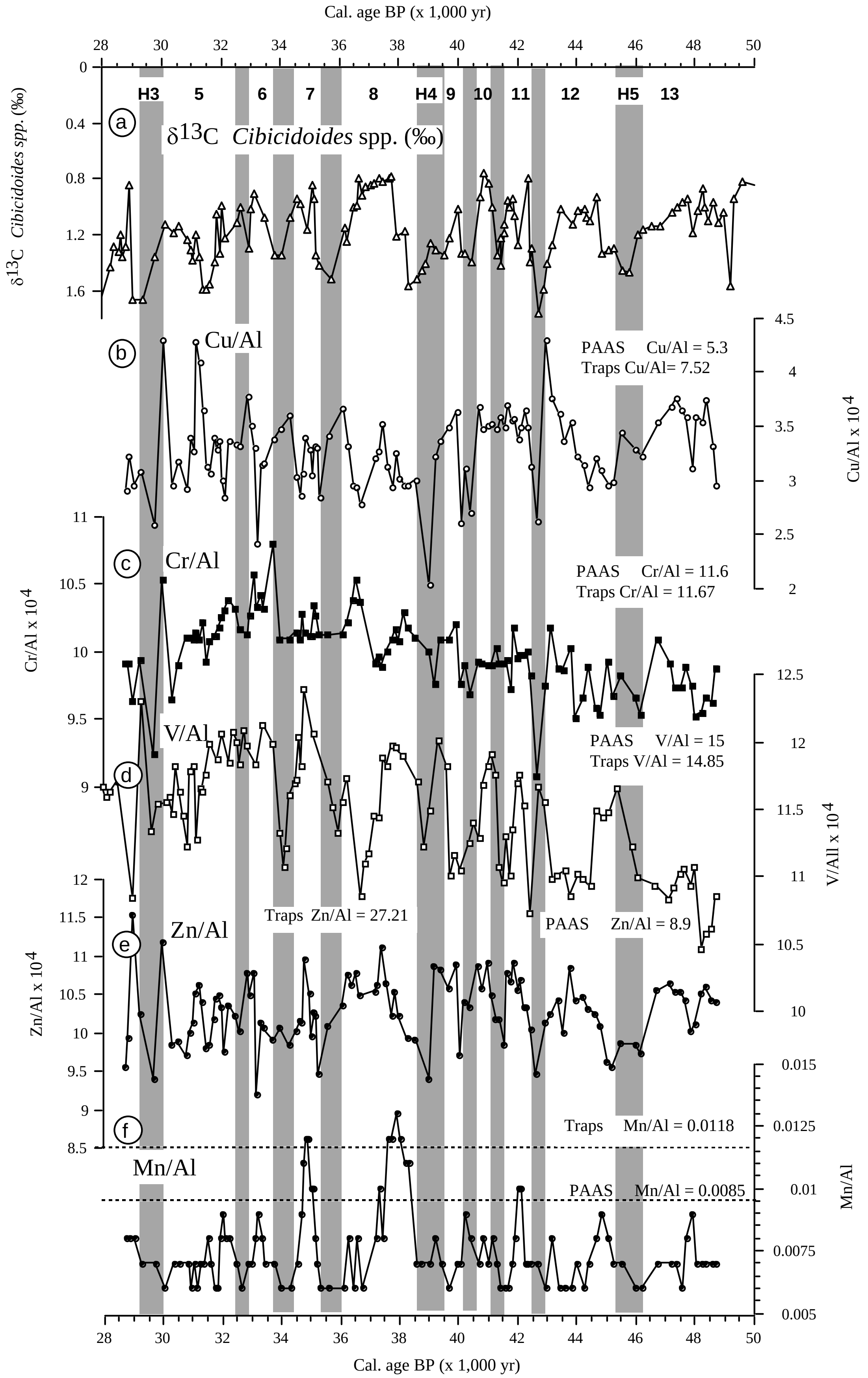

Cal. age BP (x 1,000 yr)
H3
5
6
7
8
H4
9
10
11
12
H5
13
a
δ13C Cibicidoides spp. (‰)
δ13C Cibicidoides spp. (‰)
b
Cu/Al
PAAS Cu/Al = 5.3
Traps Cu/Al= 7.52
Cu/Al x 10^4
c
Cr/Al
PAAS Cr/Al = 11.6
Traps Cr/Al = 11.67
Cr/Al x 10^4
d
V/Al
PAAS V/Al = 15
Traps V/Al = 14.85
V/All x 10^4
e
Zn/Al
Traps Zn/Al = 27.21
PAAS Zn/Al = 8.9
Zn/Al x 10^4
f
Mn/Al
Traps Mn/Al = 0.0118
PAAS Mn/Al = 0.0085
Mn/Al
Cal. age BP (x 1,000 yr)

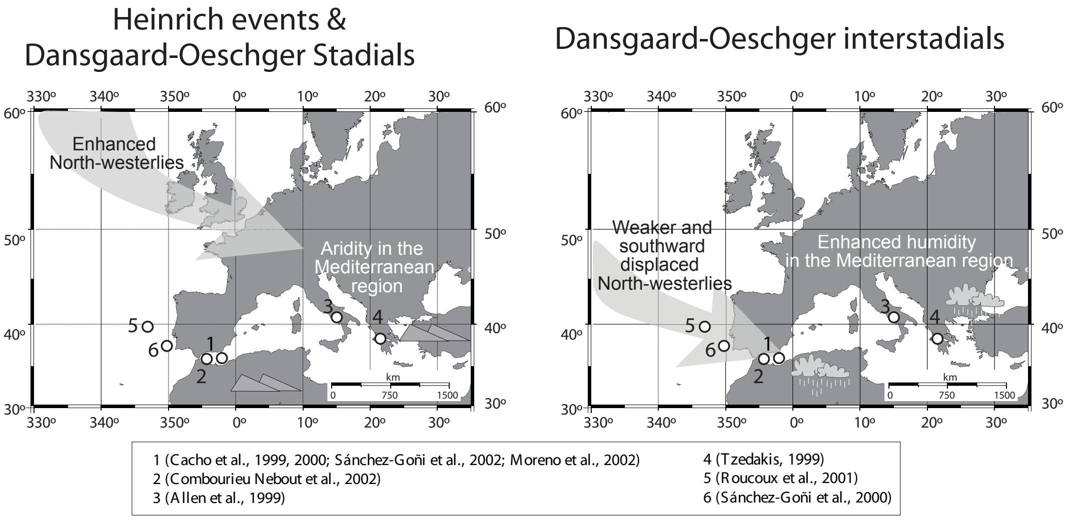
Heinrich events &
Dansgaard-Oeschger Stadials
Dansgaard-Oeschger interstadials
Enhanced
North-westerlies
Aridity in the
Mediterranean
region
Weaker and
southward
displaced
North-westerlies
Enhanced humidity
in the Mediterranean region
330º 340º 350º 0º 10º 20º 30º
60º 50º 40º 30º
km
0 750 1500
1 (Cacho et al., 1999, 2000; Sánchez-Goñi et al., 2002; Moreno et al., 2002)
2 (Combourieu Nebout et al., 2002)
3 (Allen et al., 1999)
4 (Tzedakis, 1999)
5 (Roucoux et al., 2001)
6 (Sánchez-Goñi et al., 2000)